Supplementary Information

Poly-antioxidant for enhanced anti-miR-155 delivery and synergistic therapy of metastatic breast cancer

Qingyan Zhang[#], Ying Huang[#], Ruoxi Yang, Junmei Mu, Zhanwei Zhou*, Minjie Sun*

NMPA Key Laboratory for Research and Evaluation of Pharmaceutical Preparations and Excipients, State Key Laboratory of Natural Medicines, Department of Pharmaceutics, China Pharmaceutical University, 24 Tong Jia Xiang, Nanjing 210009, P. R. China

# These authors contribute equally to this work

* Corresponding authors:
Dr. Zhanwei Zhou, Email: zwzhou@cpu.edu.cn
Prof. Minjie Sun, Email: msun@cpu.edu.cn

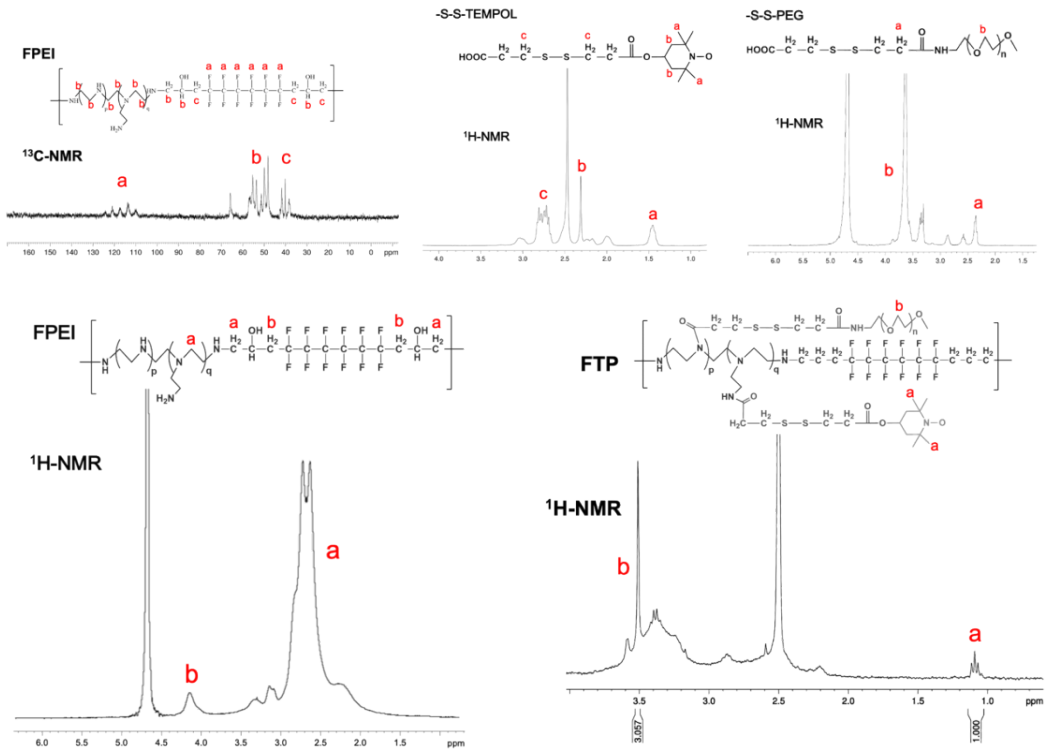

Fig. S1. ^{13}C-NMR and ^{1}H-NMR spectrum of FPEI, ^{1}H-NMR spectrum of -S-S-TEMPOL, -S-S-PEG and FTP.

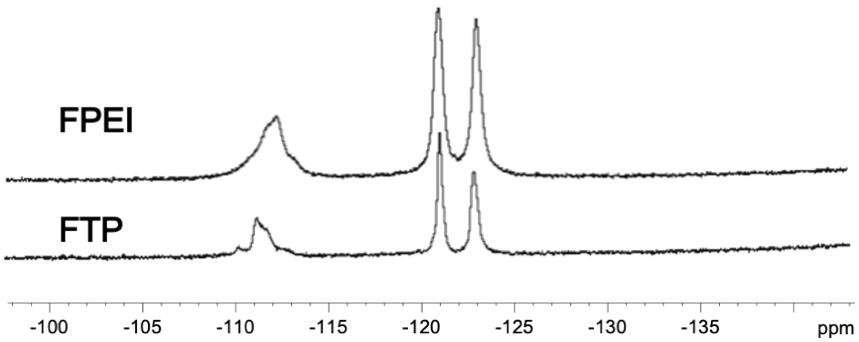

Fig. S2. ^{19}F-NMR spectrum of FPEI and FTP.

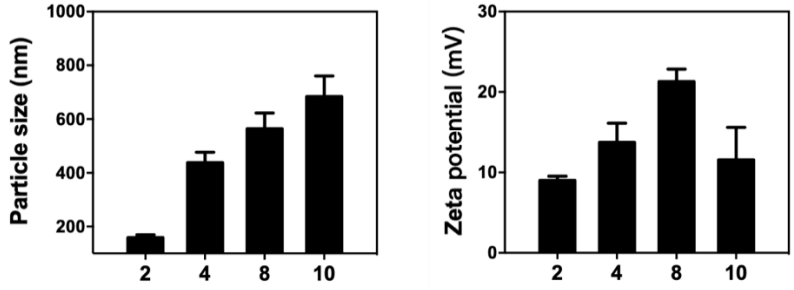

Fig. S3. Particle size and zeta potential determination of FPEI/miRNA at various w/w ratios.

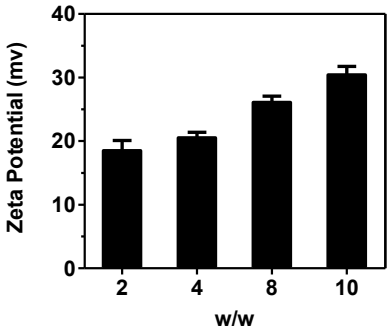

Fig. S4. Zeta potential determination of FTP/miRNA at various w/w ratios.

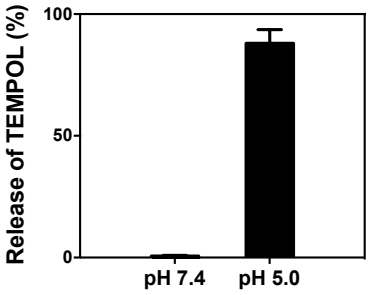

Fig. S5. The release of TEMPOL from FTP/miRNA with pH 7.4 or 5.0.

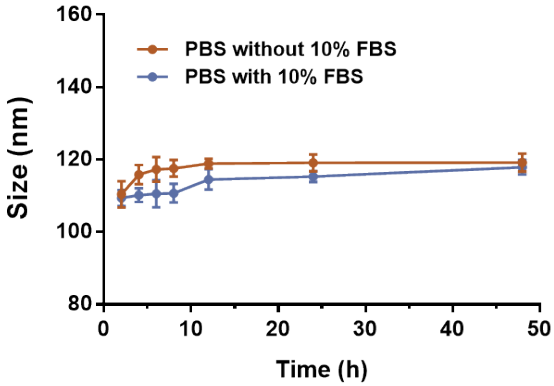

Fig. S6. The particle size changes of FTP/anti-miR-155 in PBS with or without 10% FBS.

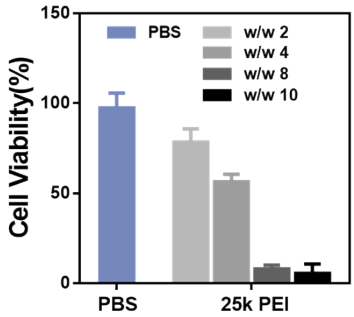

Fig. S7. Cytotoxicity of anti-miR-155 loaded 25k PEI on 4T1 cells at various w/w ratios.

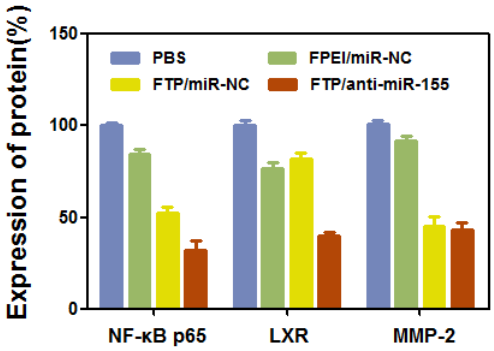

Fig. S8. Expression of NF-κB, LXR and MMP-2 in 4T1 cells determined by western blot.

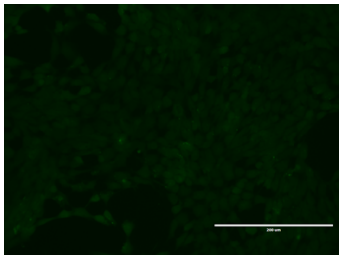

Fig. S9. Representative fluorescent image of 4T1 cells depicting ROS level after FTP treatment (scale bar, 200 μm).

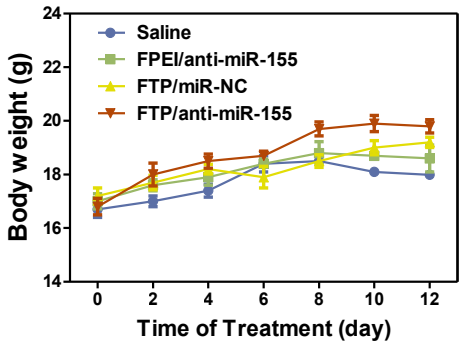

Fig. S10. Body weight monitoring during treatments (n = 6).

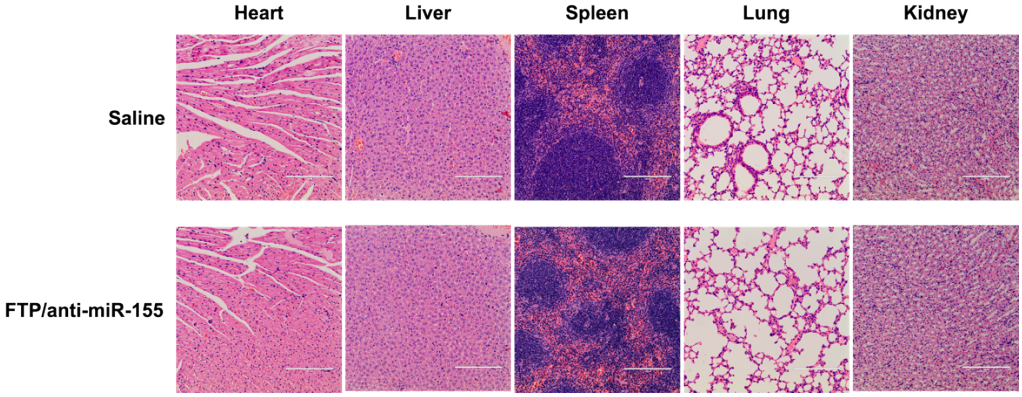

Fig. S11. H&E staining of the heart, liver, spleen, lung, and kidney after treatment with saline and FTP/anti-miR-155.